PULSATING HEAT PIPE IN HYPERGRAVITY CONDITIONS

M. Mameli,[1,3] M. Manzoni,[1] L. Araneo,[2] S. Filippeschi,[3] & M. Marengo[1,4]*

[1]*Università di Bergamo, Viale Marconi 5, 24044 Dalmine (BG), Italy*

[2]*Politecnico di Milano, Dipartimento di Energia, Via Lambruschini 4A, 20158 Milano, Italy*

[3]*Università di Pisa, DESTEC, Largo Lazzarino 2, 56122 Pisa, Italy*

[4] *School of Computing, Engineering and Mathematics, University of Brighton, Brighton BN2 4GJ, UK*

*Address all correspondence to: M. Mameli, E-mail: mauro.mameli@ing.unipi.it

1. INTRODUCTION

The present industry demand of high heat transfer capability coupled with relatively cheap component costs leads to the evolution of novel two-phase passive systems. The latent heat associated with evaporation and condensation is indeed a very efficient means of absorbing or releasing heat at relatively small temperature differences. The closed-loop pulsating heat pipe (CLPHP) is one of the most recent and

promising two-phase heat transfer devices, suitable for moderately high heat flux applications (up to 30 W/cm^2) allowing the reduction of moving mechanical elements and capable of leading up to an efficient thermal control in space.

Patented in its most common assessment by Akachi (1990, 1993), a CLPHP usually consists of a capillary diameter tube closed end-to-end, evacuated and then partially filled with a working fluid that results as an alternation of vapor bubbles and liquid slugs inside the tube. When heat power is provided to the evaporator section, the thin liquid film, which surrounds each vapor plugs, evaporates, bubbles expand and push the adjacent fluid towards the condenser zone where heat is rejected to the cold source and condensation occurs within the vapor plugs nearby the inner wall surface.

In spite of the simple structure (e.g., no porous wick structures), the PHP working principles are complex: nowadays, there are no models capable of fully describing and predicting the actual behavior of a PHP both in transient and in pseudosteady-state operation. Moreover, a reliable database which contemplates a large variety of operating conditions (e.g., gravity modifications) cannot be easily found in the literature. In particular, the behavior of a CLPHP in hypergravity has never been studied in detail, at least for a tube PHP, especially with regard to investigating the temperature trends with the thermal resistance varying the heat flux.

Except the on-going work (Ayel et al., 2013), there are only a few studies of the PHP behavior under microgravity and hypergravity conditions, available in the literature.

Experiments in normal, hyper- (2.5 g), and microgravity (0.02 g on Falcon-20 flying parabolic trajectories), conditions were performed on a flat plate pulsating heat pipe (FPPHP) charged with R114, with square channels (1.5 mm) engraved in an aluminum plate (Gu et al., 2004, 2005). One thermocouple was used to characterize the heating and cooling sections, and the device is always tested in two positions: vertical gravity assisted (bottom heated mode, BHM), and vertical antigravity (top heated mode, THM). They concluded that under normal and hypergravity conditions, the orientation affected the heat transfer performance. Moreover, under reduced gravity, the heat pipes showed a better operating and heat transport performance than when under normal and hypergravity conditions. However, on taking a careful look at the results, this last statement is evident only when the normal gravity is compared with the microgravity data obtained in the THM. Indeed, it is expected that the occurrence of microgravity is beneficial when the device is working in the antigravity mode while it is not for a gravity-assisted PHP.

A stainless steel PHP having a 1.1-mm internal tube diameter, 23 turns, and closed ends, was charged with acetone (60 vol.%) and tested on a home-made centrifuge table. Experiments were performed at different orientations with respect to the acceleration direction. The data confirm that the acceleration level influences the pressure and the corresponding temperature trends along such device (Kiseev and Zolkin, 1999).

A three-dimensional flat-plate oscillating heat pipe (3D FP-OHP) was tested under hypergravity loading with unfavorable evaporator positioning (Ma et al., 2011). The heat pipe (3.0 × 3.0 × 0.254 cm) was charged with acetone and tested with heat input of 95 W within a spin-table centrifuge. It was found that performances are near-independent of the investigated hypergravity loading up to 10 g. The results show that the thermal conductivity of the investigated device remained near-independent of gravity loading and slightly increase during the 10-g loading; clearly, these findings suggest that the device can operate in any orientation with respect to gravity, and this demonstrates a robust thermal performance.

A flat-plate PHP consisting of a serpentine channel milled in an aluminum plate covered by a thin top plate glued to the base plate partially filled with a working fluid was tested in hypergravity condition (Van Es and Woering, 2000). The experiments were focused on fluid distribution, measurements of liquid and vapor slug oscillations, and assessment of the best working fluid and filling ratio. High-acceleration experiments were carried out on a rotating table, capable of generating 8.4 g at the FSHP center. The FSHP is heated by powering dissipating elements on the hot side; cooling was achieved by means of a Peltier element at the cold side; thermocouples were fixed on several locations in the FSHP. Two experiments were performed, one with a stainless steel prototype using ethanol as a working fluid and one with an aluminum prototype filled with acetone. The experiments performed on the first prototype show a first-order increase in the evaporator temperature to a stepwise boost in acceleration after few minutes of spinning at 4.4 g. On the other hand, the second prototype was subjected to a high-g test, where the acceleration was increased to 8.4 g. The maximum temperature difference over the FSHP was approximately 22.5^{o}C and it remained constant with acceleration increase.

The thermal-gravitational modeling and scaling of two-phase heat transport systems for spacecraft applications up to 12 g was widely discussed by Delil (1999, 2000, 2001a,b). This investigation follows some previous works carried out at the Dutch National Aerospace Laboratory (NLR) on the same subject. They dealt with mechanically and capillary pumped two-phase loops. The activities pertained to pure geometric, pure fluid to fluid, or hybrid scaling between a prototype system and a model at the same gravity level, and between a prototype in gravity modified condition and a model inn normal g-level condition. However, no comparison with experimental results was made.

The objective of the present work is to study the combined effect of heat input and hypergravity level either on the closed-loop pulsating heat pipe (CLPHP) thermal performance, or on the local fluid pressure fluctuations in transient and pseudosteady-state conditions. Indeed, a 2D serpentine CLPHP made of a copper tube (O.D./I.D. = 2.0/1.1 mm) charged with FC-72 (50% filling ratio) and equipped with 13 T-type thermocouples (9 in the evaporator and 4 in the condenser) have been tested at different heat loads (50, 70, and 100 W), orientations (vertical bottom heated and horizontal), and gravity levels (from ground gravity up

to 20 g) on the European Space Agency (ESA) large-diameter cintrifuge (LDC) in Noordwijk (NL) (Van Loon et al., 2008).

2. EXPERIMENTS

2.1 Experimental Apparatus

The geometric characteristics of the PHP are briefly described in Fig. 1. The basic PHP structure consists of a copper tube having an internal diameter of 1.1 mm and external diameter of 2.0 mm folded so as to obtain thirty-two parallel channels and sixteen U-bends in the evaporator zone and then closed end to end by means of two T-joints (tin soldered). A pressure transducer (Kulite®, ETL/T 312, 1.2 bar A) is located in the condenser section. The PHP is equipped with fourteen T-type thermocouples (wire diameter 0.127 mm, accuracy $\pm 0.2^{o}$C after calibration): nine are tin soldered on the external tube surface in the evaporator and four in the condenser in order to maximize the thermal contact. The last thermocouple measures the environmental temperature. The test cell geometry as well as the thermocouples location are shown in Fig. 1.

While evacuating the PHP by means of an ultrahigh vacuum system (Varian® DS42 and TV81-T) down to $3.0 \cdot 10^{-4}$ Pa, the working fluid (FC-72) is degassed in a secondary loop by continuous boiling and vacuuming cycles. Finally the PHP is filled to a volumetric ratio of 0.5 $\pm$ 0.03 and permanently sealed by means of tin soldering. The incondensable gas content, less than 6 PPM, is estimated by meas-

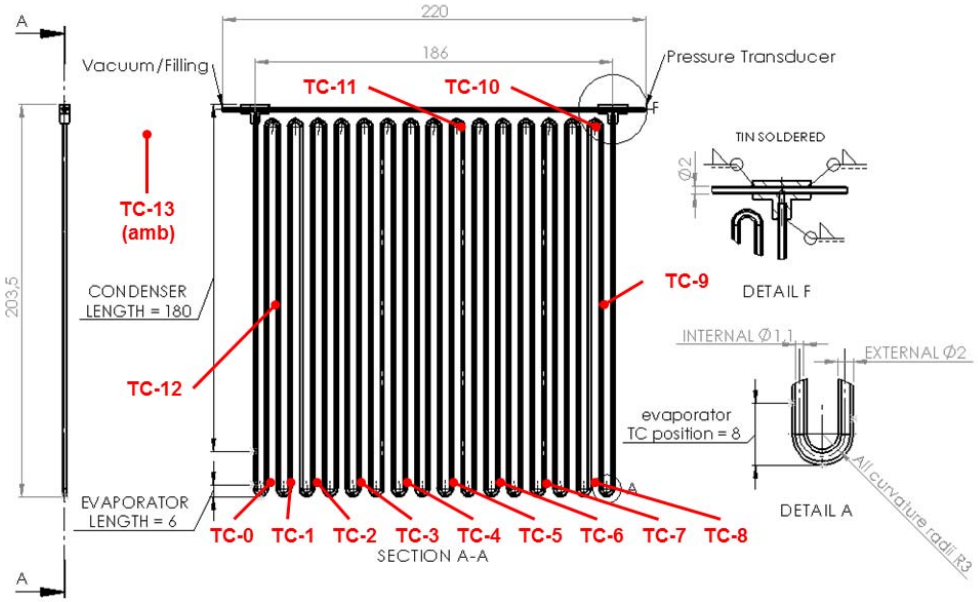

FIG. 1: Technical sketch of the PHP

FIG. 2: Heating wire wrapped on the evaporator section

uring the difference between the actual fluid pressure inside the PHP and its saturation pressure at the environmental temperature.

The PHP heater consists of 4 electric resistors connected in parallel (Thermocoax® Single core 1 Nc Ac) with a total length of 3 m, 0.5 mm external diameter, and total electrical resistance 36 Ω. The wire is wrapped around the evaporator bends, as shown in Fig. 2. The PHP evaporator and the heater are protected by a polyetheretherketone (PEEK) cover. Anyway the heaters are equipped with two thermos-fuses (DMP 11MP 150H 046E) so that the power supply is stopped whenever their temperature rises above 150^{o}C. Electric power, up to 100 W, is provided by a power supply (GWInstek® 3610A) corresponding to a radial heat flux of up to 12 W/cm^2 $\pm$ 0.3. Thermal contact is obtained by means of the heat sink compound.

The condenser section is 180-mm long and it is cooled by means of a heat sink and air fans system. Circular cross-section channels are milled on the back surface of the aluminum heat sink so as to host the copper tubes. The PHP condenser is embedded into the heat sink (Fig. 3a) and fixed with an aluminum back plate. Thermal contact is obtained by means of the heat sink compound. Four air fans (ebmpapst.co.uk® 8412N/2GH-214) are located on the heat sink fins in suction mode, as shown in Fig. 3b. The effect of the LDC acceleration on the fans rotation speed is shown in Fig. 4. The PHP in the vertical position undergoes a negligible fan speed reduction, while in the horizontal position this reduction increases with the acceleration level. The horizontal tests have been performed up to 20 g where the reduction (–12%) is critical for the cooling characteristics. Therefore only the results up to 10 g will be considered for the horizontal position.

The PHP is also equipped with a g-sensor (Analog Devices® ADXL326) located on one side of the heat sink. The thermocouples, pressure transducer, g-sensor, and the power supply are connected to a data acquisition system (NI-cRIO-9073, NI-9214®), and all signals are recorded at 16 Hz.

The test cell (PHP, thermocouples, pressure transducer, g sensor, heating and cooling system) is positioned on a beam structure by means of four antivibration bushes. Then, the structure may be fixed on the test rig plate with two different orientations: PHP vertical bottom heated, PHP horizontal, as shown in Fig. 5.

a)

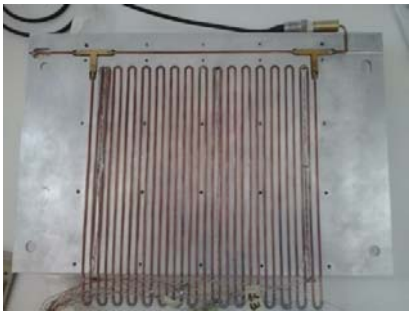

b)

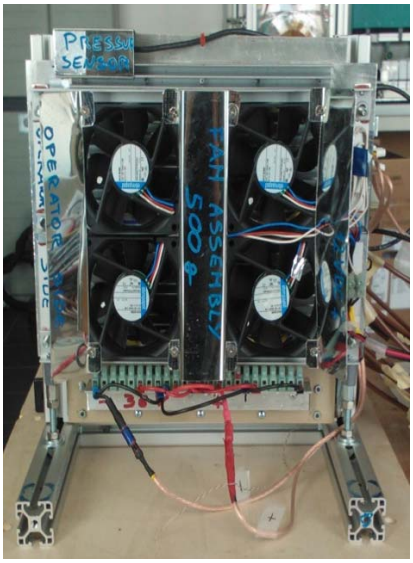

c)

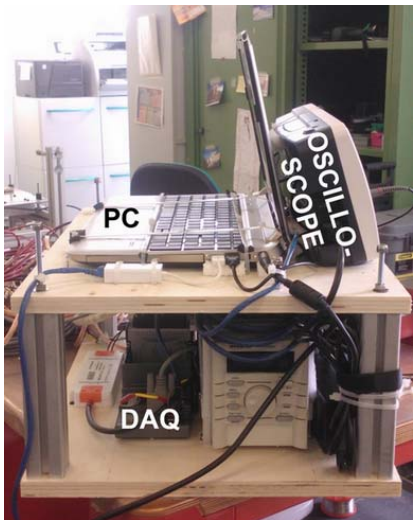

FIG. 3: a) PHP condenser section embedded into the aluminum heat sink; b) air fan system; c) peripheral facilities

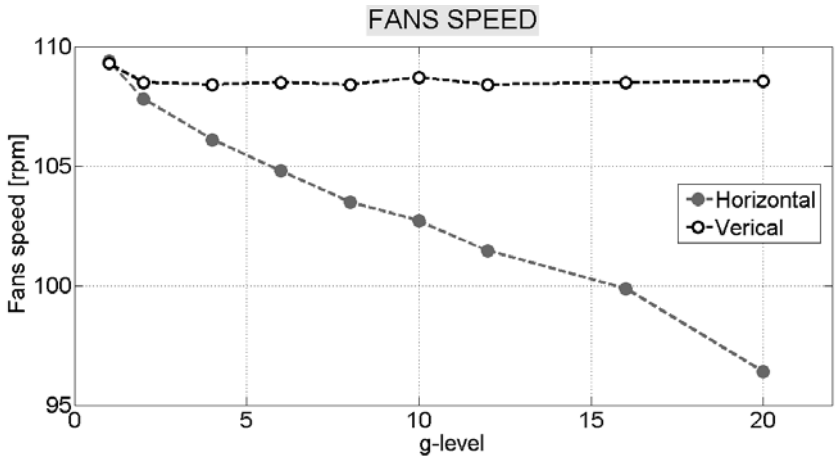

FIG. 4: Effect of the gravity level on the air fan speed

a)

b)

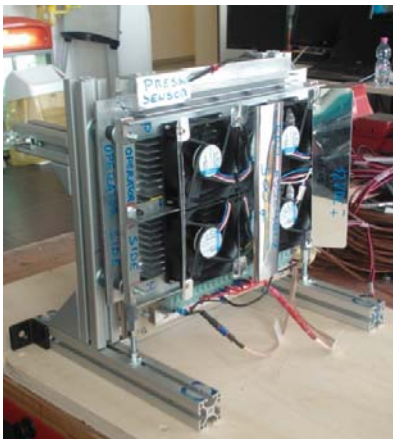

FIG. 5: Pulsating heat pipe position with respect to the gravity direction: a) horizontal; b) vertical

FIG. 6: Large-diameter centrifuge: hub and gondola

Only the PHP test cell (PHP tube, heater, condenser, and sensors) is located in the gondola (Fig. 6) while all the peripheral facilities (power supply, data logger, laptop, and oscilloscope shown in Fig. 3c) are located in the LDC hub in order to avoid hypergravity on the electronic equipment. Shielded wires (6.5-m long) then pass through the LDC branch and connect the test cell to the hardware in the hub.

There are no mechanical connections between the gondola floor and the PHP support, since the test rig is kept still and stable thanks to the gravity modified acceleration; the LDC is, indeed, a passive swing out system and the gondola will orient such that the gravity vector is always perpendicular to its floor.

2.2 Experimental Procedure

The list of both ground and hypergravity experiments is presented in Table 1. The device has been tested in two orientations with respect to the gravity direction (vertical bottom heated, horizontal) as shown in Fig. 5, at different heating power levels (50, 70, and 100 W) and different gravity levels (1, 2, 4, 6, 10, 12, 16, and 20 g).

Every experiment has been carried out in the following succession: first, the PHP test rig is arranged in vertical (bottom heated mode) or horizontal configuration and, if hypergravity is required, the PHP is placed inside an LDC gondola. Then the gondola is closed and the gravity vs. time profile is set. Afterwards, the initial heat input level is set and the experiment is powered up at normal gravity (1 g) to warm-up the PHP for at least 8 min; even though every test is performed with a peculiar gravity and heat power history, every heat input or gravity level step is then kept for 8 min (the system is able to reach the pseudosteady state, which means that all temperature signals show an average value constant in time, in about 180 s). Finally, the heating power supply is switched off and a cool down phase (15 min) is performed at the normal g-level so that all temperatures reach the room conditions. A repeatability test has been performed for almost every testing condition.

TABLE 1: List of the performed experiments

Test No.	Location	Orientation	Heat input, W	g level	Repeated
1	Ground	Horizontal	50 → 70 → 100	1	Y
2	Ground	Vertical	50 → 70→ 100	1	Y
3	LDC	Horizontal	2*x* (50 → 70 → 100 → 70 → 50)	2 → 4 → 6 → 10	Y
4	LDC	Horizontal	100	1 → 2 → 4 → 6 → 8 → 10	Y
5	LDC	Horizontal	70	1 → 4 → 8 → 10 → 12 → 16 → 20	N
6	LDC	Horizontal	50	1 → 4 → 6 → 8 → 10	N
7	LDC	Vertical	50 → 70 → 100	2	Y
8	LDC	Vertical	50 → 70 → 100	4	Y
9	LDC	Vertical	50 → 70 → 100	6	Y
10	LDC	Vertical	50 → 70 → 100	10	Y
11	LDC	Vertical	100	101 → 4 8 → 10 → 12 → 16 → 20	Y
12	LDC	Vertical	70	1 → 4 → 5 → 6 → 7 → 8 → 10 → 12	N
13	LDC	Vertical	50	1 → 2 → 3 → 4 → 5 → 6 → 8 → 10	N

3. RESULTS

The results are presented mainly in terms of temperature and pressure time evolutions. The tube wall temperature trends, both in the evaporator zone (reddish colors), condenser zone (bluish colors), and environment (green) are shown together with the heat input level on the secondary *y* axis in the above part, while the local fluid pressure in the condenser together with the heat input level on the secondary *y* axis is shown below. In the case of a centrifugal test, the gravity acceleration is reported directly over the plot line.

3.1 Ground Test

A ground test has been performed in the vertical and horizontal positions increasing the heat input from 50 W to 100 W with an intermediate step at 70 W. The starting heat input level is kept for 16 min, while the next levels are kept for 8 min each, as shown in Fig. 7. The vertical (Fig. 7a) and horizontal (Fig. 7b) orientations show very different behaviors confirming that, in a perfect 2D layout with a relatively high number of channels, gravity still exerts an important effect on the

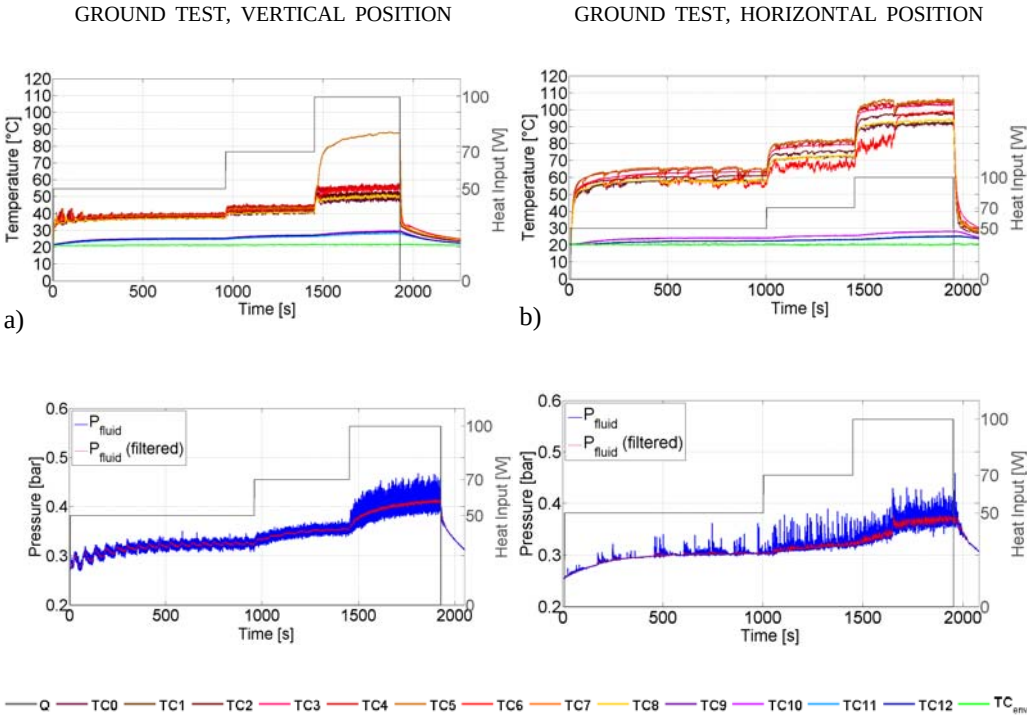

FIG. 7: Ground experiments. Tube wall temperatures and local fluid pressure in the vertical (a) and horizontal (b) positions

PHP thermal behavior. Indeed, in the horizontal working mode the fluid motion is not assisted by gravity anymore, oscillations are less frequent, the heat transfer rate is less efficient too, and, consequently, temperatures in the evaporator are set to a higher level with respect to the vertical position. After a start-up period of about 180 s, the temperatures and pressure are able to reach a regular oscillating regime. In the vertical case, the evaporator temperatures are set in a 10^{o}C range which is narrower than the horizontal one (up to 30^{o}C). The vertical operation shows an interesting feature at the higher heat input level (100 W): some channels (only one in this case) undergo a sudden thermal crisis probably due to the fluid motion dampening or local dry-out; its temperature is by more than 30^{o}C higher than all the others measured in the evaporator.

3.2 Hypergravity Test

The large-diameter centrifuge allows reaching accelerations up to 20 times the terrestrial gravity maximum. For the first time in the literature, a tube CLPHP is tested in horizontal and vertical positions at such high acceleration levels. The combined effect of heat input and gravity levels on the PHP thermal behavior is described below.

3.2.1 Horizontal position

In this case, the gravity vector is perpendicular to the flow path, thus the flow motion is not directly affected by the increasing acceleration. However, the ratio between the buoyancy forces and the surface tension forces acting on the liquid, changes with gravity and consequently the flow pattern may be altered. Indeed, in order to have an initial slug–plug distribution, the fluid confinement criterion (Balldassari and Marengo, 2013) should be satisfied (the Bond number is defined as $\mathrm{Bo} = g\,(\rho_l - \rho_v)\,D^2/\sigma$, where g is the gravity acceleration, $\rho_l - \rho_v$ is the difference between the liquid and vapor density under saturation conditions, D is the tube internal diameter, and σ is the surface tension). The critical diameter obtained by the previous criterion is plotted in Fig. 8 as a function of temperature at different acceleration levels.

The actual CLPHP internal tube diameter is plotted by a dashed line: if the critical diameter is less than the actual diameter, the fluid may not be in the confined region anymore and stratification may occur. Theoretically, Fig. 8 suggests that this transition should occur between 2 and 3 g.

Since such PHP configuration does not allow any fluid visualization, it is possible to argue about the flow transition only in terms of thermal response and local fluid pressure fluctuations. Indeed, it is here assumed that the flow regime is altered when all the temperatures in the evaporator together with the local pressure in the condenser react instantaneously to a change in the acceleration level.

The first test in the horizontal position is carried out by changing both the heat input and the gravity level. At 50 W and 1 g the device is operating in a start–stop mode, and this is clearly visible from the very poor pressure and temperature fluc-

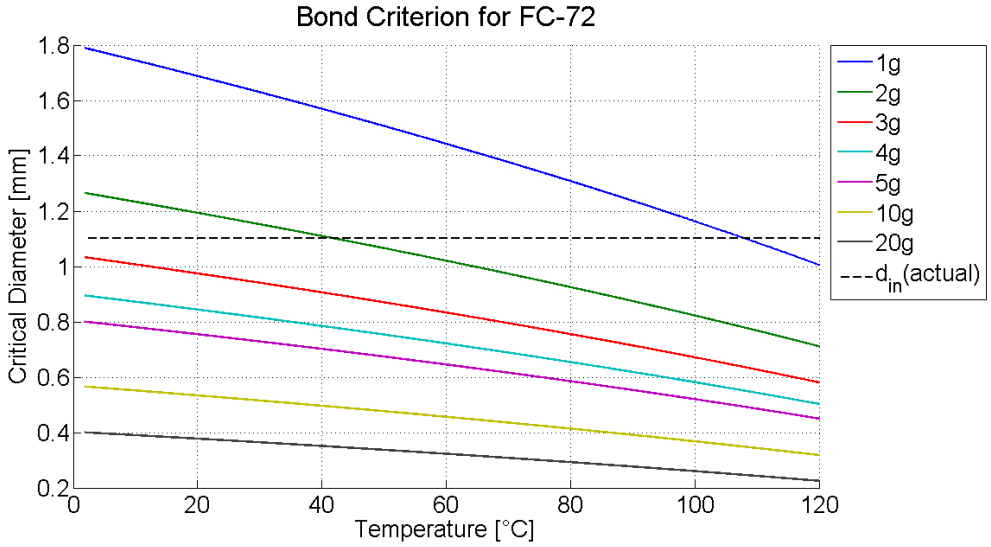

FIG. 8: Critical internal diameter as a function of temperature at different acceleration levels

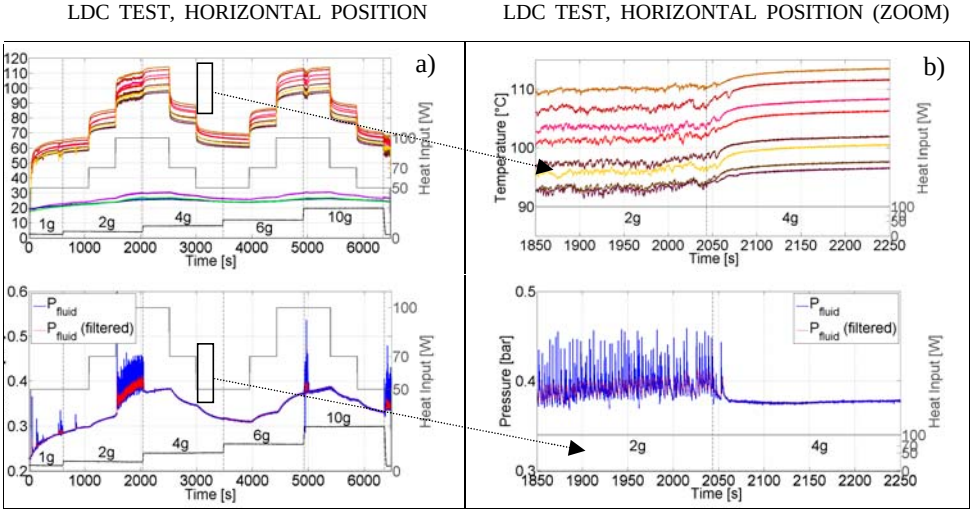

FIG. 9: Large-diameter centrifuge experiments: a) tube wall temperatures and local fluid pressure in the horizontal position at different heat inputs and gravity levels; b) zoom on the transition between 2 g and 4 g

tuation in Fig. 9a. When the gravity level is increased to 2 g, only one oscillating event is recognizable at 50 W. Keeping the spin at 2 g, the heat input level is increased to 70 W, and the fluid motion seems completely damped out: there are no signal oscillations both in the fluid pressure and wall temperatures. Only when the heat input is set at 100 W, the fluid pressure shows a higher peek, oscillation is reactivated and kept stable till the next increase in the gravity level. Indeed, when the spin is increased to 4 g the device stops working in a few seconds: the fluid pressure as well as the wall temperatures do not oscillate and the thermal performance slightly decreases, as shown in Fig. 9b. Afterwards, the heat input level is decreased to 70 W and then to 50 W at 4 g but no reactivation occurred, as expected.

For the next duty cycle, gravity is increased to 6 g and, again, the heat input level is increased from 50 W to 100 W. Only a sudden pressure peek is recorded at 100 W during the transition from 6 to 10 g but, contrary to the 2 g case, it is only a local event, not sufficient to restart the device operation. No operation is detected afterwards in hypergravity but, when the LDC stops and the gravity level gets back to 1 g, the PHP recovers a vigorous temperature and pressure oscillation. The experiment has been repeated and no substantial differences arose.

In order to verify the hysteresis effect linked to the heating/gravity history, tests are performed at increasing acceleration levels, keeping the heat input at the evaporator constant. As expected from the results shown in Fig. 9, both tests at 50 and 70 W show that the PHP stops working when the gravity changes from 1 to 4 g but the switching off is almost instantaneous at 50 W (Fig. 10a), while almost one minute is needed at 70 W (Fig. 10b). Differently, if the heat input level is kept at 100 W since the very beginning, the PHP is able to maintain a stable operation up to 4 g

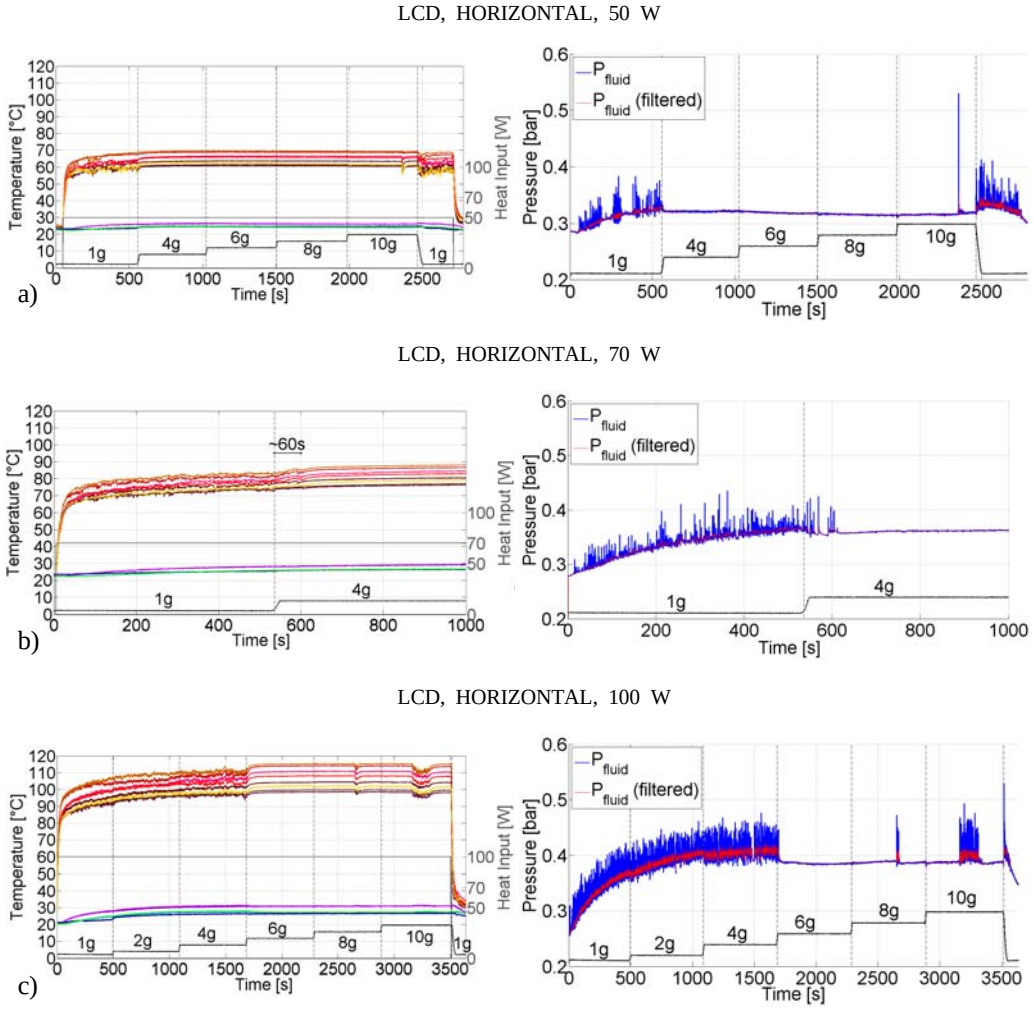

FIG. 10: Large-diameter centrifuge experiments. Tube wall temperatures and local fluid pressure in the horizontal position and at different gravity levels at: a) 50 W; b) 70 W; c) 100 W

showing, by comparison with Fig. 9, a dependence on the heating/gravity history. Local fluid settlements occur at 8 g and at 10 g but, as in the previous experiments, the local event is not sufficient to restart the device operations. Hypergravity test have been performed up to 20 g at 70 W but results are shown only for up to 4 g because no PHP operation have been recorded above this gravity level.

3.2.2 Vertical position

When the PHP is oriented in the vertical bottom heated position, the acceleration vector is parallel to the flow path direction. The vertical experiments are carried

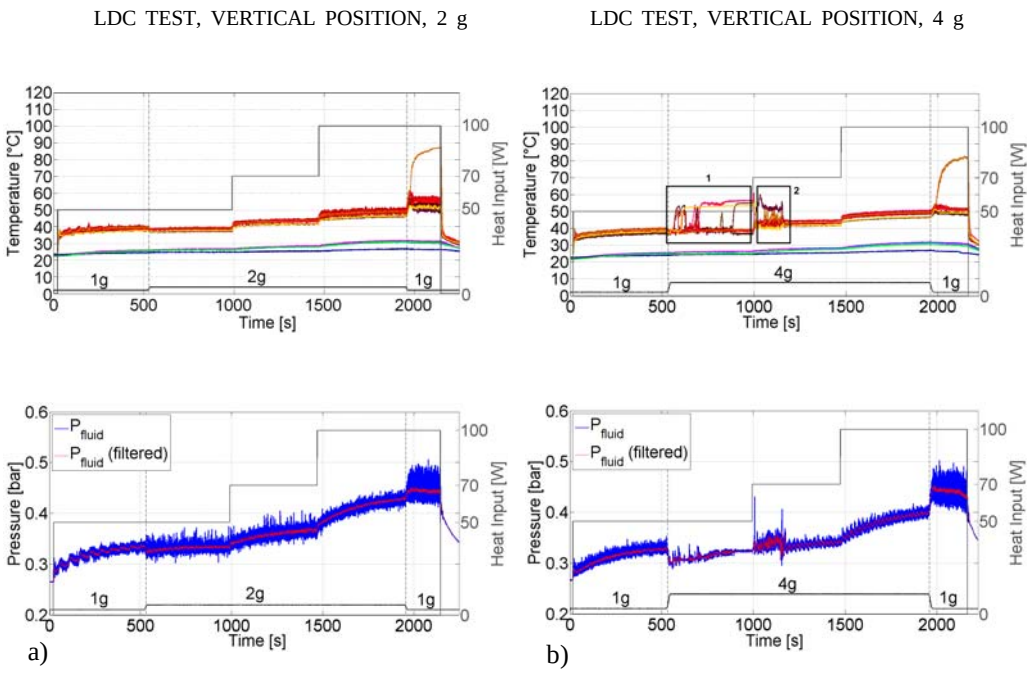

FIG. 11: Large-diameter centrifuge experiments. Tube wall temperatures and local fluid pressure in the vertical position and at different heat input levels at: a) 2 g; b) 4 g

out in order to understand to what extent the gravity may assist or inhibit the flow motion. The device is started up at 50 W in normal gravity conditions till the pseudosteady state is reached, then the same heating cycle (50, 70, and 100 W) is performed at constant gravity levels. Figure 11a shows that the PHP is working with slightly better thermal performance at 2 g: the average evaporator temperature can be directly compared between 1 g and 2 g for 50 W and 100 W and in both cases it is evidently lower. Furthermore, the 2 g acceleration prevents the occurrence of local dry-outs at 100 W: all the evaporator temperatures are within a narrow range till the LDC stops and the ochre temperature signal rises identically to the ground test. These results are comparable with those achieved with the same apparatus in the hypergravity phases (1.8 g) during the 58th ESA Parabolic Flight Campaign (Mameli et al., 2014). Figure 11b shows that at 4 g acceleration strongly inhibits the fluid motion, as shown by the pressure diagram, at 50 W and many locations in the evaporator undergo local fluid dry-outs and temperature increase (thermal crisis — zone 1).

At 70 W another kind of thermal instability occurs, characterized by a more frequent stopover phenomenon and resulting in large amplitude and less regular temperature and pressure oscillations, (transient thermal instability — zone 2). Nevertheless the system is able to resettle, after about 120 s, and afterwards it kept a stable and efficient operation. No local thermal instabilities are detected at 100 W, too.

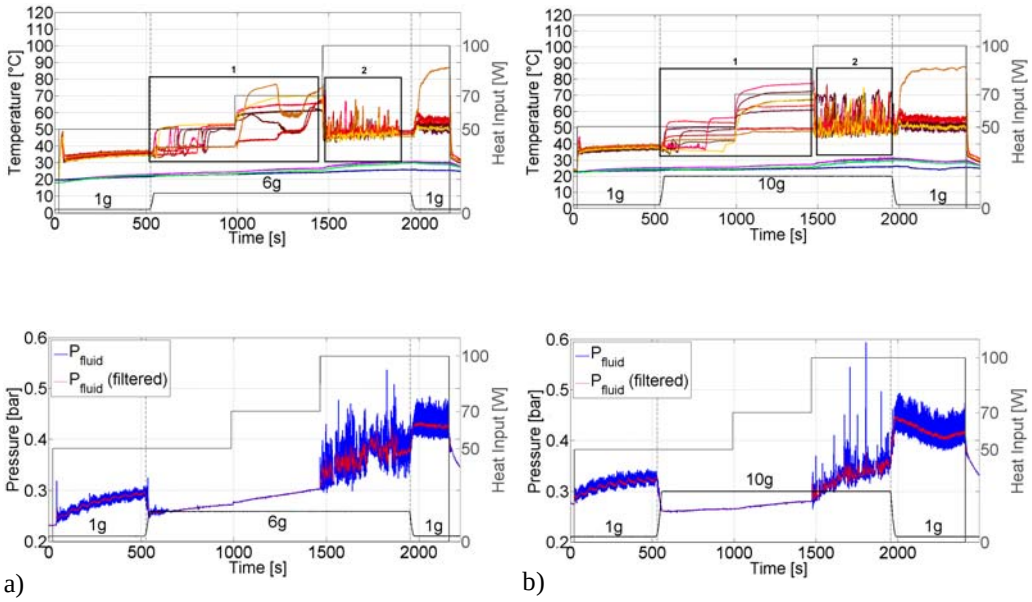

FIG. 12: Large-diameter centrifuge experiments. Tube wall temperatures and local fluid pressure in the vertical position and at different heat input levels at: a) 6 g; b) 10 g

At 6 g (Fig. 12a), the first unstable zone 1 covers a wider heat input range: neither the 50 W nor the 70 W heat input levels provide enough thermal driving force to promote a stable fluid oscillation. Only at 100 W, the vapor expansion is strong enough to compete with the gravity acceleration. Indeed, after a long settlement period characterized by frequent stopovers phenomena and large amplitude temperature and pressure oscillations (zone 2), a stable behavior is finally reached. At 10 g (Fig. 12b), zone 1 covers the 50 W and 70 W period as for the 6 g test but, at 100 W, the device is not able anymore to recover from the second transient thermal instability. As for the horizontal case, additional tests are performed increasing acceleration levels and keeping the heat input constant (Fig. 13). As expected, the two different thermal instabilities detected in the previous test (zones 1 and 2) occur in these experiments, too. Moreover, like the horizontal mode, the performances of the PHP seem to be slightly dependent on the heating/gravity history. For example, the two tests performed at the same heat input level, 70 W, but coming from different heating/gravity paths (Figs. 12a and 13a), show that the PHP respectively undergoes two different thermal instabilities at 6 g.

A peculiar behavior can be observed for the PHP powered with 50 W: at 4 g, after a very small period of transient thermal instability (zone 2), the device undergoes a very long thermal crisis (zone 1) and the number of dried-out channels increase with the acceleration level but, interestingly, their temperature level slightly

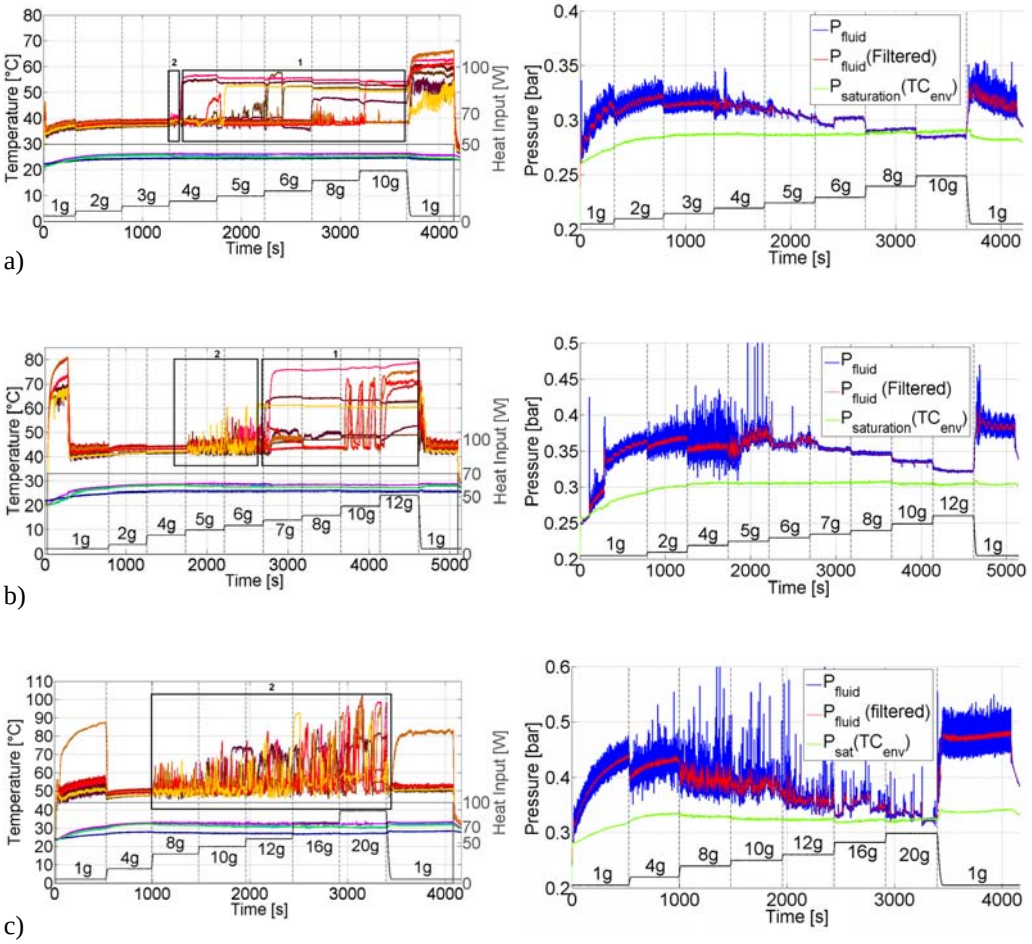

FIG. 13: Large-diameter centrifuge experiments. Tube wall temperatures and local fluid pressure in the vertical position and at different gravity levels at: a) 50 W; b) 70 W; c) 100 W

decreases. Furthermore, when the LDC stops spinning, the PHP is not able to recover the stable operation. At 70 W, as expected, the transition between 1, 2, and 4 g enhances the performances of the PHP. Then at 5 and 6 g a transient thermal instability occurs driving the PHP to a complete thermal crisis regime. This is comparable with what has been previously observed for 50 W. Therefore, it seems that the transient thermal instability is, actually, a transition between a stable mode (where performances are also enhanced by the hypergravity) and a thermal crisis regime. Note that at 100 W, the transition between zone 2 and zone 1 is not so evident, at least for the tested gravity levels.

Figure 13b shows also the theoretical fluid saturation pressure calculated as a function of the environmental temperature (green line). If the fluid is not moving

inside the condenser, its temperature will approach the cooling medium temperature. In terms of pressures, this means that the local fluid pressure approaches the saturation pressure at room temperature and the PHP is going towards worse working conditions. This is indeed what happens at increasing accelerations after the thermal crisis.

Despite the fact that internal flow visualizations could not be performed during the present experimental campaign, a possible physical explanation of the above phenomenon may be deduced on the basis of the fluid local pressure. When the PHP is working in the vertical bottom heated mode, the gravity force helps the liquid phase to flow from the condenser section to the evaporator zone. This alternation of evaporation and condensation assists the motion of the fluid inside the capillary tube and, at normal gravity, an alternation of liquid slug and vapor plugs could be achieved. A small increase of the gravity improves the performances of the PHP while, if gravity increases too much, the liquid phase is forced to flow in the evaporator section but the heating power is not any more sufficient to push it up in the condenser. This leads to the formation of a liquid storage in the bottom of the device and vapor amasses in the top section. Since the heating power is provided in the evaporator, bubbles may be still generated within the liquid storage causing a local and more chaotic fluid motion observed in the pressure signal that is oscillating in a less regular way with respect to the stable operation. Temperature in the evaporator section also undergoes unstable and incoherent oscillations (zones 2, transient thermal instability). The bubbles generated by the boiling process, however, are inhibited by a further increase of the gravity acceleration until the system reaches the overall thermal crisis (zones 1). In this case, pressure oscillations are damped and moreover, when the gravity increases, the pressure signal shows a step reduction comparable with the gravity step enhancement. Finally, it is assumed that at very high gravity levels bubbles collapse as soon as they are formed because of the very high hydraulic pressure. In this condition, the system reaches an equilibrium state, and saturation pressure can be measured in the top vapor.

4. CONCLUSIONS

A multiturn closed-loop PHP with a standard 2D geometry has been experimentally investigated on ground and in hypergravity conditions on a large-diameter centrifuge at ESA-ESTEC. The temporal trend of the wall temperature in several locations (evaporator and condenser) and the local fluid pressure signal show that the PHP thermal response is strongly and rapidly affected by the variation of the gravity field. In particular, the following salient points arise:

- On ground, vertical and horizontal orientations show very different behaviors confirming that, in a perfect 2D layout with a relatively high number of channels, the device orientation with respect to gravity still exhibits an important effect on the PHP thermal behavior.

- For the horizontal orientation, fluid stratification and the consequent thermal crisis should occur between 2 g and 3 g, on the only basis of the Bond number criterion. Instead, experiments show that the device operation stops at different acceleration levels depending also on the heat input power level and on the heating/gravity history.
- During the vertical operation, the gravity either assists or inhibits the flow motion depending on the combined effect of gravity and heat input level.
- The vertical PHP thermal performance is slightly enhanced by the lower hypergravity levels (up to 3 g at 50 W, up to 4 g at 70 W, and up to 6 g at 100 W).
- Two different local thermal crises affect the PHP thermal behavior in the vertical position: if the fluid pumping forces resulting from the heating power can compete with the acceleration forces, the system only undergoes local frequent stopover phenomena (transient thermal instability), while increasing with the acceleration level, the pumping forces are completely damped in some channels, the relative wall temperature increases and settles to a higher level (thermal crisis). A possible physical explanation of this phenomenon has been provided and supported by the condenser pressure diagram.

ACKNOWLEDGMENTS

The authors acknowledge ESA's Spin You Thesis! program organizers and LIS engineers. Thanks to the Msc thesis student Corrado Roncelli for helping in the experimental assessment. The authors would like to thank Dr. Olivier Minster and Dr. Balazs Toth for their interest and support to the PHP activities and for the fruitful discussions. Finally we acknowledge all the members of the Pulsating Heat Pipe International Scientific Team, led by Prof. Marco Marengo, for their contribution to pushing the PHP technology for real space applications, with a particular gratitude to Prof. Sameer Khandekar, Dr. Vadim Nikolayev, and Dr. Vincent Ayel.

REFERENCES

Akachi, H., Structure of a heat pipe, US Patent 4,921,041, 1990.

Akachi, H., Structure of micro-heat pipe, US Patent 5,219,020, 1993.

Ayel, V., Thevenot, F., Bertin, Y., and Romestant, C., Analyse thermo-hydraulique expérimentale d'un caloduc oscillant sous champ de gravité variable, *Congrès Français de Thermique*, SFT 2013, Gerardmer, du 28 au 31 mai, 2013.

Baldassari, C. and Marengo M., Flow boiling in microchannels and microgravity, *Prog. Energy Combust. Sci.*, vol. **39**, issue 1, pp. 1–36, 2013.

Delil, A. A. M, Scaling of two-phase heat transport systems from micro-gravity to super-gravity levels, *Proc. Space Technology and Applications International Forum*, Albuquerque, USA, pp. 221–229, 2001a.

Delil, A. A. M., Microgravity Two-Phase Flow and Heat Transfer, NLR-TP-99429, 2001b.

Delil, A. A. M., Pulsating and Oscillating Heat Transfer Device in Acceleration Environment from Microgravity to Supergravity, NLR-TP-2001-001, 1999.

Delil, A. A. M., Thermal-Gravitational Modeling and Scaling of Heat Transport Systems for Applications in Different Gravity Environments: Super-Gravity Levels and Oscillating Heat Transfer Devices, NLR-TP-2000-213, 2000.

Gu, J., Kawaji, M., and Futamaca, R., Effect of gravity on the performance on pulsating heating pipe, *J. Thermophys. Heat Transfer*, vol. **18**, no. 3, pp. 370–378, 2004.

Gu, J., Kawaji, M., and Futamaca, R., Microgravity performance of micro pulsating heating pipe, *Microgravity Sci. Technol.*, vol. **XVI**, no. 1, pp. 15–20, 2005.

Kiseev, V. M. and Zolkin, K. A., The influence of acceleration on the performance of oscillating heat pipe, *Proc. 11th Int. Heat Pipe Conf.*, pp. 154–158, Tokyo, Japan, 1999.

Ma, H., Thompson, S. M. , Hathaway, A. A., Smoot, C. D., and Wilson, C. A., Experimental investigation of a flat-plate oscillating heat pipe during high-gravity loading, Proc. *ASME 2011 Int. Mechanical Engineering Congress and Exposition IMECE2011-64821*, Denver, Colorado, USA, 2011.

Mameli, M., Araneo, L., Filippeschi, S., Marelli, L., Testa, R., and Marengo, M., Thermal response of a closed loop pulsating heat pipe under variable gravity field, *Int. J. Thermal Sci*., vol. **80**, pp. 11–22, 2014.

Van Es, J. and Woering, A. A., High-Acceleration Performance of the Flat Swinging Heat Pipe, NLR-TP-2000-265, 2000.

Van Loon, J. J. W. A., Krouse, J., Kunha, U., Goncalves, J., Almeida, H., and Schiller, P., The large diameter centrifuge, LDC, for life and physical sciences and technology, *Proc. of the Life in Space for Life on Earth Symposium*, 22–27 June 2008, Angers, France (ESA SP-663, December 2008), 2008.